

Sequential deformation and physiological considerations in unipolar right or left ventricular pacing

Oliver J. Liakopoulos^a, Hideyuki Tomioka^a, Gerald D. Buckberg^{a,b,*},
Zhongtuo Tan^a, Nikola Hristov^a, George Trummer^a

^a Department of Surgery, Division of Cardiothoracic Surgery, David Geffen School of Medicine at University of California Los Angeles, 10833 Le Conte Avenue, 62-258 CHS, Los Angeles, CA 90095-1741, USA

^b Option on Bioengineering, California Institute of Technology, Pasadena, CA, USA

Received 22 February 2006; accepted 28 February 2006

Abstract

Objective: To determine the effects of ventricular pacing on the normal contraction sequence of the helical ventricular myocardial band, and its' impact on left ventricular function. **Methods:** Ten pigs (25–68 kg) underwent analysis of percent segmental shortening (%SS) by sonomicrometry, with crystals placed along the fiber orientation of the ascending and descending segments, and posterior LV wall of the geometry of the helical heart. Unipolar pacing electrodes stimulated either the right atrium (RA), right ventricular apex (RVA) and outflow tract (RVOT), or posterior LV wall. Systemic hemodynamics, QRS-interval, cardiac index (CI), systolic and diastolic LV function and pressure–dimension (*P–D*) loops were analyzed and cardiac motion was monitored by video analysis. **Results:** Normal sinus heart rate (NSR) was elevated from 84 ± 15 beats/min to 113 ± 22 beats/min by pacing ($p < 0.05$). The variables of NSR were not changed by atrial pacing. Conversely, compared with NSR, ventricular pacing (RVA, RVOT, LV) significantly ($p < 0.05$) prolonged the QRS-interval ($94\text{--}111$ ms vs 52 ± 7 ms, $p < 0.05$) decreased mean arterial pressure ($46\text{--}47$ mmHg vs 62 ± 11 mmHg), CI ($2.7\text{--}3.4$ L/(min m²) vs 4.9 ± 0.9 L/(min m²)) and systolic LV pressure ($56\text{--}61$ mmHg vs 92 ± 10 mmHg). Furthermore, ventricular pacing decreased peak (+)d*P*/d*t* and (–)d*P*/d*t* ($p < 0.05$) and lowered PRSW to 59–77%, with most profound change after RVA pacing ($p < 0.05$). Each ventricular pacing intervention decreased SS% significantly in the descending, ascending, and posterior LV segments compared with NSR. Disruption of the normal NSR sequence of shortening (progression from descending to posterior to ascending regions) followed each pacing intervention. Changes were characterized by premature stimulation of the segment adjacent to the pacer stimulus, with associated (1) decrease of pressure–dimension loop area, (2) desynchronization of *P–D* loops and (3) consistent loss of the twisting pattern of visible cardiac motion. **Conclusions:** Ventricular pacing disrupts the natural sequence of shortening along the myocardial band, and the resultant dyssynchrony impairs LV function.

© 2006 Elsevier B.V. All rights reserved.

Keywords: Ventricular pacing; Helical myocardial ventricular band; Ventricular function; Helical heart; Sonomicrometry

1. Introduction

The normal cardiac rhythmic–contractile sequence is a twisting activity caused by sequentially organized deformation of cardiac fibers [1]. Interruption of this pattern by heart block from either natural or surgical causes is treated by pacing the right ventricular apex (RVA), a traditional method because of ease of implantation and stability [1,2]. While heart rate is restored, physiologic studies show that right ventricular apex stimulation causes abnormal cardiac function [3,4] as a consequence of asynchronous contraction. This observation has led to development of alternate pacing sites (right ventricular outflow tract (RVOT) or left ventricular (LV)) for electrical stimulation in patients with heart block

and/or bradycardia [2], especially when congestive heart failure is present [5,6]. In spite of progress in evaluating myocardial function at the hemodynamic and electrophysiological levels [7–9], the influence of different pacing sites on the organized synchrony of contraction has not yet been defined.

To accomplish this structure–function analysis, a testing model that reflects normal ventricular geometric form is needed, from which responses from different pacer stimulation sites can be compared. This study employs sonomicrometer crystals to evaluate electro-mechanical responses at different right and left ventricular locations along the myocardial band described by Torrent-Guasp [10,11]. The helical heart configuration in this model suggests that fiber shortening progresses along a sequential normal contractile wave, with maximal organized shortening developing along a principle axis aligned with left ventricle (LV) local fiber bundle orientation [10,12,13]. The underlying hypothesis is

* Corresponding author. Tel.: +1 310 206 1027; fax: +1 310 825 5895.
E-mail address: gbuckberg@mednet.ucla.edu (G.D. Buckberg).

that dyssynchrony happens when the pacing fiber stimulation causes abrupt nonsequential shortening that disrupts this normal pattern.

In the intact heart, the structural configuration of the myocardial band includes a circumferential basal loop to surround the left and right ventricles that then becomes an oblique double helix to form the apical loop [14–16]. This myocardial band forms the basal loop in continuity with the apical loop that consists of an oblique descending and an ascending segment (Fig. 1). Sequential contraction along this band determines the motion composed of narrowing (basal loop), twisting to eject and reciprocal twisting to initiate suction during the isovolumetric contraction phase of the cardiac cycle.

Stimulation sites will include the RVA and RVOT, as well as the left ventricle muscle to mimic the individual univentricular pacing sites used to generate the excitation phase for ventricular contraction. The relative value of each site is currently conjectural, as different investigators report either improvement or limited change in function after stimulation of either of these three locations [17–20]. This study is not intended to try to solve this dilemma, but rather to determine if such regional unipolar stimulation interferes with the natural sequence existing after supraventricular stimulation from either sinus rhythm or atrial pacing.

We hypothesized that stimulation of any these ventricular sites might reduce effective ventricular muscle performance compared with either regular rhythm or atrial pacing. The concept is that generation of premature sequential contraction of apical loop structures within the myocardial band would disrupt the natural deformation sequence responsible for the hemodynamic and pressure–dimension functional components of function in normal pig hearts.

2. Materials and methods

All animals received humane care in compliance with the 1996 NRC Guide for the Care and Use of Laboratory Animals, available at: <http://www.nap.edu/readingroom/books/lab-rats/contents.html>.

Ten Yorkshire–Duroc pigs (25–68 kg) were premedicated with ketamine hydrochloride (15 mg/kg) and diazepam

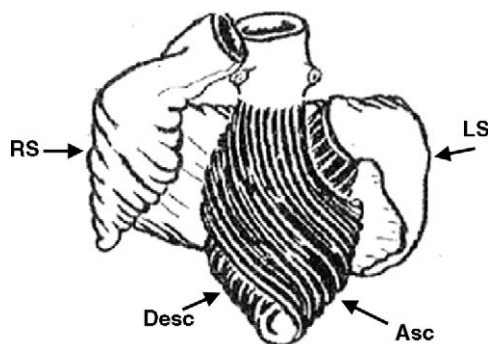


Fig. 1. The ventricular myocardial band as described by Torrent-Guasp. The basal loop (in white color) comprises a right (RS) and left segment (LS). The apical loop (in black color) is formed by a descending (Desc.) and an ascending (Asc.) segment. The oblique double helix forms an apical loop with an apical vortex.

(0.5 mg/kg) intramuscularly and anesthetized with inhaled isoflurane 1.5% (MAC 1%) throughout the operation. Support with a volume-controlled ventilator (Servo 900C, Siemens-Elcoma, Sweden) was started after tracheotomy and endotracheal intubation. FiO_2 and tidal volumes were adjusted to maintain a PaO_2 above 100 mmHg and PaCO_2 in a range of 30–40 mmHg. Arterial pressure was measured after cannulation of the femoral artery. A Swan–Ganz catheter was inserted into the pulmonary artery via the right jugular vein to measure pulmonary artery pressure (PAP), pulmonary capillary wedge pressure (PCWP) and cardiac output (thermodilution technique).

The pericardium was incised after median sternotomy and a solid-stated pressure transducer-tipped catheter (Model MPC-500, Millar Instruments Inc., Houston, TX, USA) was inserted into the left ventricle via the apex. Regional contractility within the left ventricle was measured with pairs of 2 mm ultrasonic microtransducer crystals (Sonometrics, London, Ont., Canada). Each pair of crystals was placed in order to measure contractility at certain myocardial depth and orientation. In the helical heart model described by Torrent-Guasp, cardiac muscular structures produce two simple loops that start at the pulmonary artery and end in the aorta. These components include a horizontal basal loop that surrounds the right and left ventricles, changes direction through a spiral fold in the ventricular myocardial band to cause a ventricular helix produced by oblique fibers. The oblique double helix, consisting of a descending and an ascending segment, forms an apical loop with a vortex at the left ventricular tip (Fig. 1). Four pairs of anterior left ventricular crystals, as described previously [10], were inserted into the proximal and distal (toward apex) descending segments at 80° and 90° angulation, and into the ascending segments at 140° and 160° angulation to achieve maximal shortening and to compare LV mid and apical walls (Fig. 2). A crystal pair was placed into the LV posterior wall, in a transverse direction, and perpendicular to the long axis of the left ventricle.

Unipolar pacing electrodes were positioned at following locations: the right atrium (RA), the right ventricular apex (RVA), and the right ventricular outflow tract (RVOT) and the posterior LV (Fig. 2). The indifferent electrode was placed on the chest wall of the animals. The unipolar plunge electrode consisted of an insulator, which is electrically active only at a 1 mm tip. The pacing electrodes were inserted subendocardially, as practiced by standard fashion in the clinical setting. Postmortem autopsy examination confirmed crystal and electrode placements in each study.

Sonomicrometer crystals data, aortic pressure, left ventricular pressure (LVP), the derivative of LVP (dP/dt), and lead II of the electrocardiogram (ECG) were digitally processed by specific hardware and software (Sonometrics, London, Ont., Canada). The synchronicity of myocardial contractility was matched to left ventricular performance with 1 ms recording precision through real-time plotting and processing of segment shortening, ECG, LVP, and dP/dt . Sequential contraction of different segments of the heart was then established and compared with ventricular hemodynamics during pacing from each site. In some studies, an octopus traction device was placed on the LV apex,

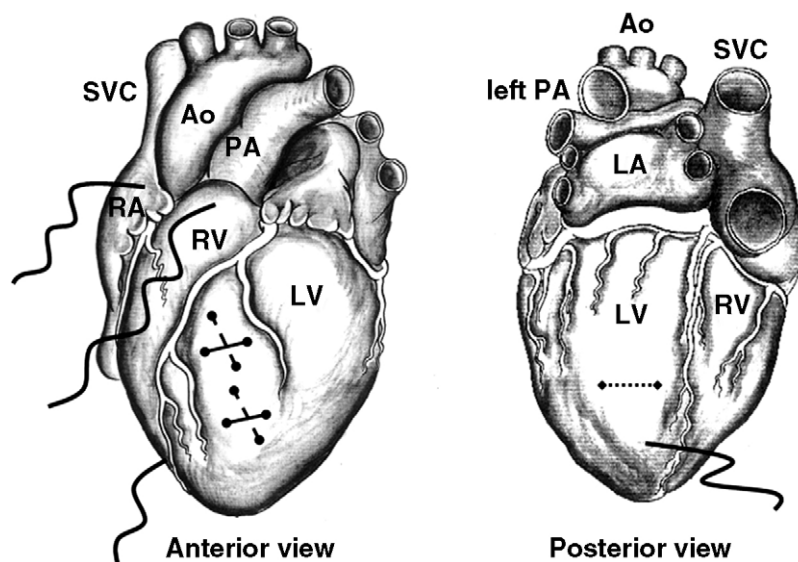


Fig. 2. Schematic anterior and posterior view of the heart showing the different pacing sites and the positioning of the sonomicrometer crystals. Unipolar pacing electrodes (wavy lines) were placed at right atrium (RA), right ventricular apex and outflow tract, and the left ventricle (LV). Crystals were placed into the posterior LV wall (◆◆◆), and the proximal and distal descending (●—●) and ascending (● - - - ●) segments of the LV free wall. Ao: aorta; LA: left atrium; PA: pulmonary artery; SVC: superior vena cava.

allowing recording of video studies to show the effectiveness of intrinsic rhythm and pacing on ventricular twisting.

2.1. Pacing protocol

A square-wave constant-voltage electronic stimulator at 2.5 times threshold stimulated the heart. Stimulation parameters (voltage, duration, and frequency) were held constant in each pig, and the mean pacing heart rate for the group was 113 ± 22 beats/min. The following pacing interventions were performed in random order: pacing of the RA, RVA, RVOT and posterior LV wall for 10 min. Hemodynamic data and pressure–dimension (P – D) and volume (P – V) loops were obtained at the end of each pacing protocol during stable hemodynamics. The pacing site was switched from one site to the other after a 10-min pause, to insure stable hemodynamic parameters between pacing protocols.

2.2. Data analysis

Electrocardiogram from limb lead II measured QRS intervals. Measurement of regional left ventricular segmental shortening of the descending and ascending segment and the posterior LV was performed as described by Castella et al. [10] and by using sonomicrometer crystals. Percentage of segmental shortening (SS%) was calculated as follows:

$$\frac{EDL - ESL}{EDL} \times 100$$

where EDL is end-diastolic length and ESL is end-systolic length.

LV dimensions were measured by two pairs of crystals oriented across the minor and major axes of the left ventricle and using a two-axis ellipsoid-based formula. Left ventricular pressure and volume were recorded for subsequent 8–12 beats during transient inferior vena cava occlusions to obtain a series of evenly declining pressure–volume loops. The end-

systolic elastance (E_{es}) was determined from the slope of the end-systolic pressure–volume line of the P – V loops. Global stroke work was calculated, and preload recruitable stroke work (PRSW) for each pacing site was identified as the relation between stroke work and end-diastolic dimension and quantified by using a slope (M_w) and x-intercept (L_w). The slope ($\times 10^3$ erg/cm³) is known to measure myocardial performance independent of loading, geometry, and heart rate [21]. LV performance for each pacing site was expressed as percentage change to control before inducing each pacing.

2.3. Statistical analysis

All data are expressed as the mean \pm standard deviation (SD). Analysis of the data was performed by paired Student's t -tests comparing each ventricular pacing site with its control. The level of significance was chosen as $p < 0.05$.

3. Results

3.1. Hemodynamics

Hemodynamic data in Table 1 contrasts sinus rhythm (NSR) against atrial, right and left ventricular pacing, and demonstrates maintenance of the normal QRS complex with atrial pacing, and QRS prolongation following ventricular pacing. Atrial pacing, despite an intrinsically higher rate than NSR, maintained MAP, LVPsys and cardiac index. In contrast, ventricular pacing from either the RVA, RVOT, or left ventricle widened QRS, reduced cardiac index, and lowered LVPsys without changing PAP, PCWP or LVEDp pressure levels.

3.2. Left ventricular function

Systolic function shows that atrial pacing maintains the highest peak (+)dP/dt (Table 2). During right and left

Table 1
Hemodynamic data during sinus rhythm and different pacing sites

	NSR	Atrial pacing	RVA pacing	RVOT pacing	LV pacing
HR (beats/min)	84 ± 15	113 ± 22 [*]	113 ± 22 [*]	113 ± 22 [*]	113 ± 22 [*]
QRS intervals (ms)	52 ± 7	48 ± 10	94 ± 3 ^{*,#}	100 ± 14 ^{*,#}	111 ± 10 ^{*,#}
MAP (mmHg)	62 ± 11	64 ± 8	47 ± 4 ^{*,#}	46 ± 6 ^{*,#}	47 ± 9 ^{*,#}
LVPsys (mmHg)	92 ± 10	85 ± 9	61 ± 7 ^{*,#}	57 ± 8 ^{*,#}	56 ± 14 ^{*,#}
PAPsys (mmHg)	22 ± 3	24 ± 6	23 ± 10	23 ± 10	21 ± 4
PCWP (mmHg)	10 ± 1	11 ± 1	11 ± 1	11 ± 1	10 ± 1
CI (L/(min m ²))	4.9 ± 0.9	4.9 ± 1.0	2.7 ± 0.6 ^{*,#}	3.2 ± 0.6 ^{*,#}	2.8 ± 0.3 ^{*,#}

Hemodynamic data during normal sinus rhythm (NSR) and pacing of the right atrium (RA), left ventricle (LV), right ventricular apex (RVA) and outflow tract (RVOT). HR: heart rate; MAP: mean arterial pressure; LVPsys: left ventricular systolic pressure; PAPsys: pulmonary artery systolic pressure; PCWP: pulmonary capillary wedge pressure; CI: cardiac index. All data are mean ± SD.

^{*} $p < 0.05$ compared to NSR.

[#] $p < 0.05$ compared to atrial pacing.

ventricular pacing, peak (+)dP/dt fell, but tended to be slightly better during RVOT and LV pacing than RVA pacing. Right and left ventricular pacing lowered end-systolic elastance (E_{es}) as compared with NSR and atrial pacing, with the most profound lowering after RVA pacing. Right atrial pacing slightly decreased PRSW values to $89 \pm 17\%$ of NSR baseline values, but further reduction followed RVOT ($77 \pm 32\%$), LV ($65 \pm 9\%$) and RVA pacing ($59 \pm 25\%$) compared with baseline ($p < 0.05$).

Diastolic function analysis (Table 2) indicated that atrial pacing maintained the highest peak (–)dP/dt, whereas the extent of reduced negativity was greater during RVA than LV and RVOT pacing.

3.3. Changes in segmental shortening (SS%)

During NSR, SS% ranged from 15.4 ± 2.6 in the descending segment to 14.5 ± 1.8 in the ascending segment and

18.8 ± 6.1 in the posterior wall, with approximately 27% more shortening in the distal than proximal left ventricular free wall position (Table 3). Right atrial pacing slightly decreased regional SS% compared with NSR. Conversely, right and left ventricular pacing decreased SS% of each site, with the most profound depression following RVA pacing (Table 3).

3.4. Sequential contraction of the left ventricle

In normal sinus rhythm (NSR), a time-delay existed between the beginning and end of shortening of the ascending and descending segments. The normal sequence of shortening during NSR is shown in Fig. 3, displaying (a) initial LV anterior wall shortening of the descending segment corresponding to Q-wave of the ECG and early slow LVP rise, (b) LV posterior wall shortening starting 14 ± 8 ms later, and (c) LV ascending segment shortening (corresponding with peak positive dP/dt wave and S-wave on ECG recording)

Table 2
Results of pacing interventions on systolic and diastolic function

	NSR	Atrial pacing	RVA pacing	RVOT pacing	LV pacing
Peak (+)dP/dt (mmHg/s)	1199 ± 321	1251 ± 244	836 ± 280 ^{*,#}	924 ± 193 ^{*,#}	915 ± 226 ^{*,#}
E_{es} (mmHg/mm)	4.2 ± 2.0	3.7 ± 1.7	3.2 ± 1.8 [*]	3.4 ± 1.7 [*]	3.3 ± 2.4 [*]
PRSW (%)	100	89 ± 17	59 ± 25 ^{*,#}	77 ± 32 [*]	65 ± 9 ^{*,#}
Peak (–)dP/dt (mmHg/s)	–1274 ± 247	–1344 ± 355	–675 ± 248 [*]	–753 ± 225 [*]	–689 ± 162 [*]
LVEDP (mmHg)	14 ± 3	13 ± 2	10 ± 2	10 ± 2	10 ± 2

Systolic and diastolic parameters during normal sinus rhythm (NSR) and pacing of the right atrium (RA), left ventricle (LV), right ventricular apex (RVA) and outflow tract (RVOT). Peak (+)dP/dt: peak positive first derivative of LVP; E_{es} : end-systolic elastance; PRSW: preload recruitable stroke work; peak (–)dP/dt: peak negative first derivative of LVP; LVEDP: left ventricular end-diastolic pressure. All data are mean ± SD.

^{*} $p < 0.05$ compared to NSR.

[#] $p < 0.05$ compared to atrial pacing.

Table 3
Influence of pacing interventions on segmental shortening (SS%)

	Proximal Desc.	Distal Desc.	Proximal Asc.	Distal Asc.	Post. LV
NSR	15.4 ± 2.6	20.1 ± 6.4	14.5 ± 1.8	15.6 ± 2.1	18.8 ± 6.1
Atrial pacing	13.1 ± 2.1	16.6 ± 5.9 [*]	12.3 ± 3.3	12.9 ± 3.4	16.8 ± 6.2
RVA pacing	11.9 ± 3.3 [*]	16.5 ± 7.1 [*]	9.0 ± 2.1 ^{*,#}	9.2 ± 3.1 ^{*,#}	13.9 ± 7.7 [*]
RVOT pacing	12.3 ± 2.9 [*]	15.8 ± 8.0 [*]	9.3 ± 1.1 ^{*,#}	10.0 ± 1.4 ^{*,#}	13.6 ± 9.6 [*]
LV pacing	11.9 ± 2.5 [*]	16.3 ± 6.7 [*]	9.1 ± 2.0 ^{*,#}	9.1 ± 2.1 ^{*,#}	13.9 ± 8.9 [*]

Percentage of segmental shortening (SS%) during normal sinus rhythm (NSR) and pacing of the right atrium, right ventricular apex (RVA), RV outflow tract (RVOT), and left ventricle (LV). Proximal/distal Desc.: proximal and distal SS% of the descending segment of the apical loop; proximal/distal Asc.: proximal and distal SS% of the ascending segment of the apical loop; Post. LV: SS% of the posterior wall of the left ventricle. All data are mean ± SD.

^{*} $p < 0.05$ compared to NSR.

[#] $p < 0.05$ compared to atrial pacing.

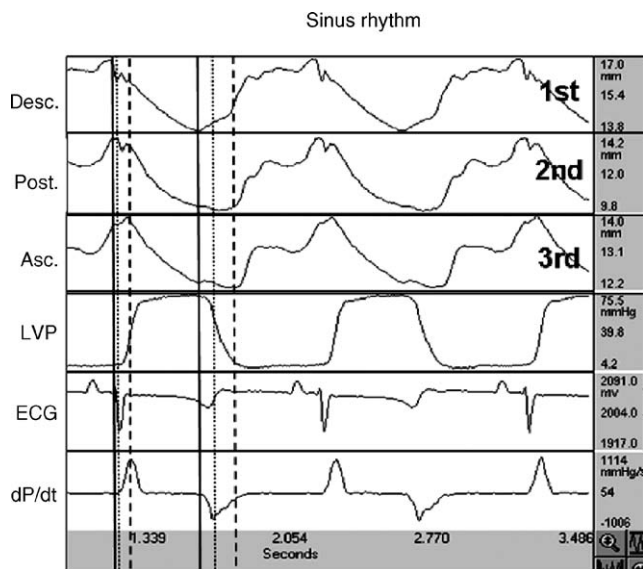


Fig. 3. Simultaneous recordings of sequential shortening of the descending (Desc.), posterior (Post.) and ascending (Asc.) segments during NSR. Note, the normal sequence of shortening (a) starts with shortening of the descending segment corresponding to early slow LVP rise, (b) followed by the posterior LV wall shortening 14 ± 8 ms later, and (c) finally LV ascending segment shortening corresponding with peak positive dP/dt wave, 86 ± 14 ms after shortening of descending segment. Furthermore, end of shortening showed a similar pattern with end of shortening first at the descending segment, followed by the posterior and then by the ascending segment. Marking lines indicate the start and end of shortening in the descending segment (solid line), posterior wall (punctuated line) and ascending segment (hatched line). LVP: left ventricular pressure; ECG: electrocardiogram; dP/dt: first derivate of LVP.

beginning 86 ± 14 ms after endocardial (descending) segment shortening. Furthermore, the end of shortening followed a similar pattern, cessation of posterior and ascending segments were 20 ± 12 ms and 110 ± 2 ms, respectively, after the descending segment shortening had stopped. The cardiac motion showed a twisting pattern during NSR by visual examination and as depicted in Video 1 (Appendix A).

This sequential shortening behavior pattern was maintained with atrial pacing (Fig. 4), as was the twisting visual appearance on Video 2 (Appendix A), although timing intervals shortened due to the more rapid heart rate following atrial pacing. In contrast, ventricular pacing produced marked aberration in the shortening pattern compared with supraventricular activation. Early shortening consistently existed in regions close to the pacemaker site and late shortening in regions more remote from the ventricular pacing site (Figs. 5–7).

Pacing of the LV produced an early start and end of shortening of the posterior LV segment which occurred almost simultaneously with the descending segment, followed by the ascending segment (Fig. 5). Video analysis showed a consistent loss of the twisting pattern of cardiac motion (Video 3 (Appendix A)). RVA pacing resulted in (a) shortening of the descending endocardial segment immediately at the R-spike of the ECG rather than during the initial slope of LVP rise, (b) shortening of the ascending epicardial segment 5 ± 10 ms after shortening of the endocardial segment, but before posterior wall shortening, (c) delayed posterior LV wall shortening to begin 80 ± 10 ms after endocardial

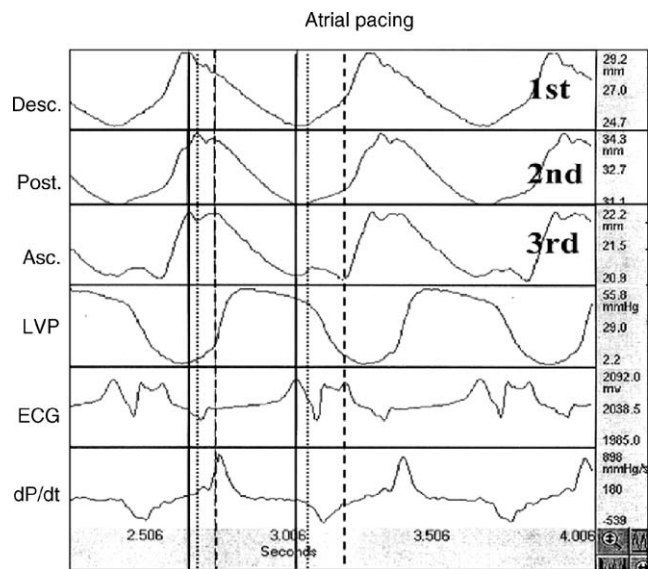


Fig. 4. Simultaneous recordings of sequential shortening of the descending (Desc.), posterior (Post.) and ascending (Asc.) segments during pacing of the right atrium. Note that with atrial pacing the sequence of shortening of the segments was maintained compared with normal sinus rhythm, with a decrease of time intervals between segments due to a higher heart rate. Marking lines indicate the start and end of shortening in the descending segment (solid line), posterior wall (punctuated line) and ascending segment (hatched line). LVP: left ventricular pressure; ECG: electrocardiogram; dP/dt: first derivate of LVP.

segment shortening (Fig. 6). These changes resulted in a loss of the twisting pattern of the ventricle as shown by Video 4 (Appendix A).

Another nonsequential pattern existed during RVOT pacing (Fig. 7), whereby (a) endocardial shortening had a normal contraction pattern, but (b) epicardial shortening

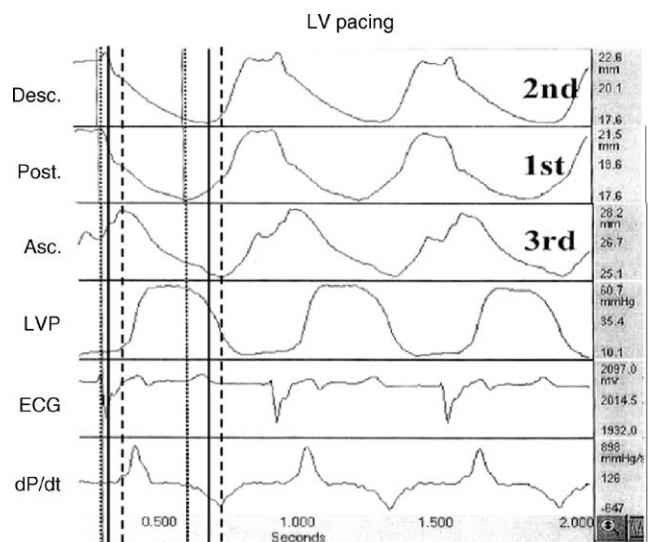


Fig. 5. Simultaneous recordings of sequential shortening of the descending (Desc.), posterior (Post.) and ascending (Asc.) segments during pacing of the left ventricle (LV). Note that LV pacing produced an early start and end of shortening of the posterior LV segment which occurred almost simultaneously with the descending segment, followed by the ascending segment. Marking lines indicate the start and end of shortening in the descending segment (solid line), posterior wall (punctuated line) and ascending segment (hatched line). LVP: left ventricular pressure; ECG: electrocardiogram; dP/dt: first derivate of LVP.

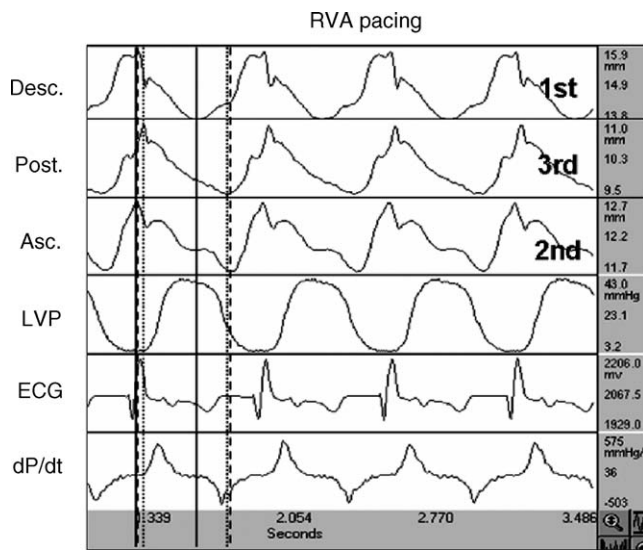


Fig. 6. Simultaneous recordings of sequential shortening of the descending (Desc.), posterior (Post.) and ascending (Asc.) segments during pacing of the right ventricular apex (RVA). Note, the marked aberration in the shortening pattern among all segments with (a) shortening of the descending segment immediately at the R-spike of the ECG rather than during the initial slope of LVP rise, (b) shortening of the ascending epicardial segment 5 ± 10 ms after shortening of the endocardial segment, but before posterior wall shortening, and (c) delayed posterior LV wall shortening after endocardial segment shortening. Marking lines indicate the start and end of shortening in the descending segment (solid line), posterior wall (punctuated line) and ascending segment (hatched line). LVP: left ventricular pressure; ECG: electrocardiogram; dP/dt: first derivative of LVP.

occurred almost simultaneously with the descending segment, and (c) LV posterior wall contracted after both segments of the LV anterior free wall started contraction. Additionally, the normal cardiac motion and visual twisting was abolished as shown in [Video 5 \(Appendix A\)](#). An alternate shortening pattern during RVOT pacing was observed in a different specimen ([Fig. 8](#)), where the timing sequence seemed to follow the order observed following atrial pacing.

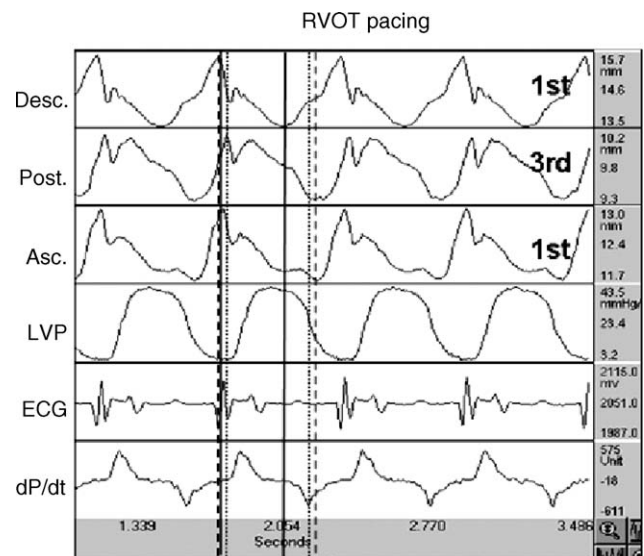


Fig. 7. Simultaneous recordings of sequential shortening of the descending (Desc.), posterior (Post.) and ascending (Asc.) segments during pacing of the right ventricular outflow tract (RVOT). Note that (a) endocardial (descending segment) shortening had a normal contraction pattern, but (b) epicardial shortening occurred almost simultaneously with the descending segment, and (c) LV posterior wall contracted after both segments of the LV anterior free wall started contraction. Marking lines indicate the start and end of shortening in the descending segment (solid line), posterior wall (punctuated line) and ascending segment (hatched line). LVP: left ventricular pressure; ECG: electrocardiogram; dP/dt: first derivative of LVP.

However, there was a disruption of how this sequence affected the initial slow rise of LV pressure. Instead of the normal response of coincidental slow rise, the pressure curve was flattened, presumably due to desynchronization of how pacing effected the pressure–dimension relationship.

Furthermore, ventricular pacing caused differences in sequential shortening interaction between endocardial and epicardial crystal pairs in proximal LV and distal (apex)

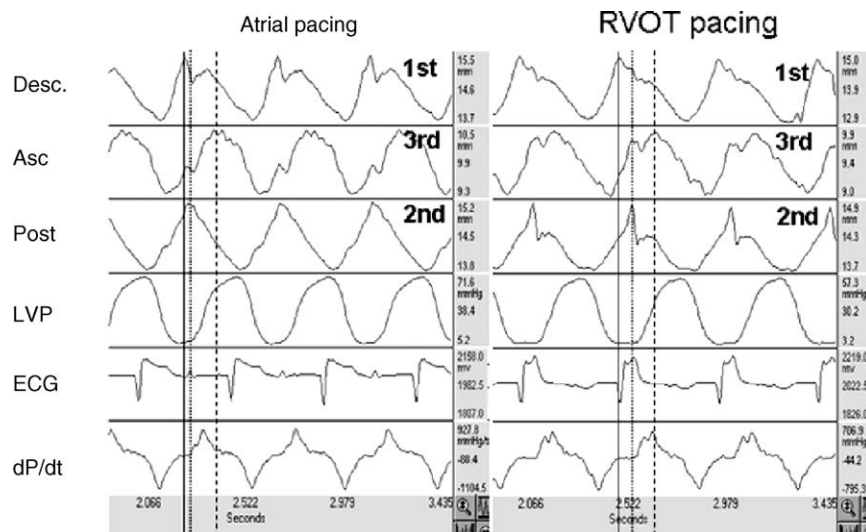


Fig. 8. Recordings of a different shortening pattern during RVOT pacing. Note the onset of shortening during RVOT pacing, commenced in both the descending segment (solid line) and the posterior wall (punctuated line), is markedly out of phase with LVP compared with atrial pacing because of too early onset of shortening. LVP: left ventricular pressure; ECG: electrocardiogram; dP/dt: first derivative of LVP.

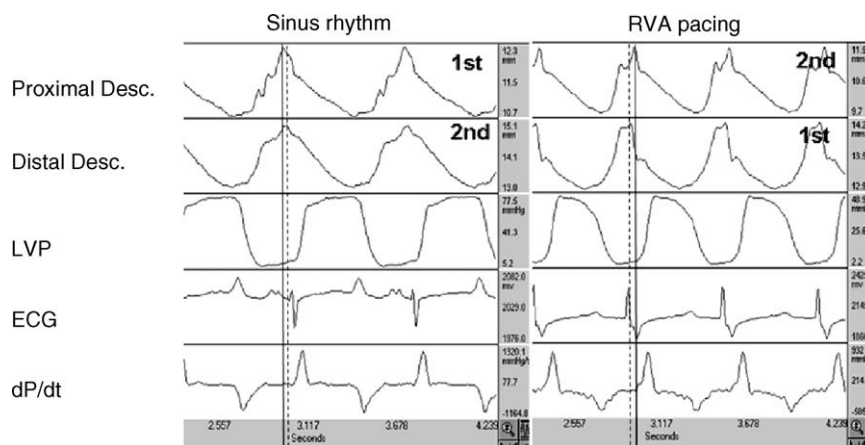


Fig. 9. Comparison of the sequence of shortening between the proximal (solid line) and the distal (hatched line) portion of the descending segment during NSR and RVA pacing. Apical RV pacing inverted the sequence of shortening with the distal portion of the descending segment starting earlier than the proximal. LVP: left ventricular pressure; ECG: electrocardiogram; dP/dt: first derivative of LVP.

positions (Fig. 9). Apical contraction occurred before contraction of the proximal descending segment and visual twisting was disrupted after RVA pacing (Video 4). This sequence differed from to atrial pacing, where the onset of the proximal descending segment shortening preceded distal descending segment shortening. This pattern was reversed also by RVOT pacing, as the region closest to the pacing site *always* shortened earliest.

3.5. Pressure–dimension loops

Pressure–dimension (P – D) loops provided a more detailed insight into regional function of the different segments during pacing interventions. P – D loops during NSR and atrial pacing showed a similar pattern, with start of contraction of

the descending segment at the beginning of the initial slow rise of LVP (Fig. 10A and B). This was followed by shortening of the LV posterior wall segment, which occurred during the rapid rise of LVP, and finally the ascending segment contraction was started at the end of LVP rise during systolic ejection of the ventricle. The P – D loops of the apical loop segments and posterior wall showed a timing pattern at the end of contraction, whereby the descending segment stopped first, followed by the LV posterior wall, and finally by the ascending segment.

In contrast to the findings during supraventricular rhythm, ventricular pacing (Fig. 11A–C) produced marked aberrations in the P – D loops of all segments, and was most pronounced during RVA pacing. Stroke work, as indicated by the integrated area of P – D loops, was decreased in the apical

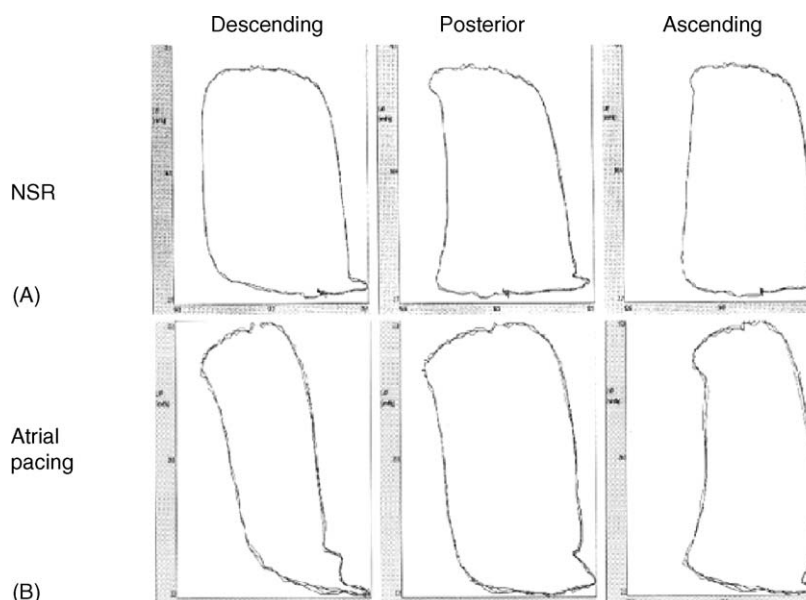


Fig. 10. Comparison of the pressure–dimension (P – D) loops of the descending, posterior and ascending segments during NSR and atrial pacing. The longitudinal axis expresses LV pressure (mmHg), and horizontal axis is segment length (mm). Note that (a) P – D loops during NSR (A) and atrial pacing (B) showed a similar pattern, with start of contraction of the descending segment at the beginning of the initial slow rise of LVP, followed by the start of shortening of the LV posterior wall segment and finally the start of contraction of the ascending segment at the end of LVP rise during the systolic ejection phase of the ventricle.

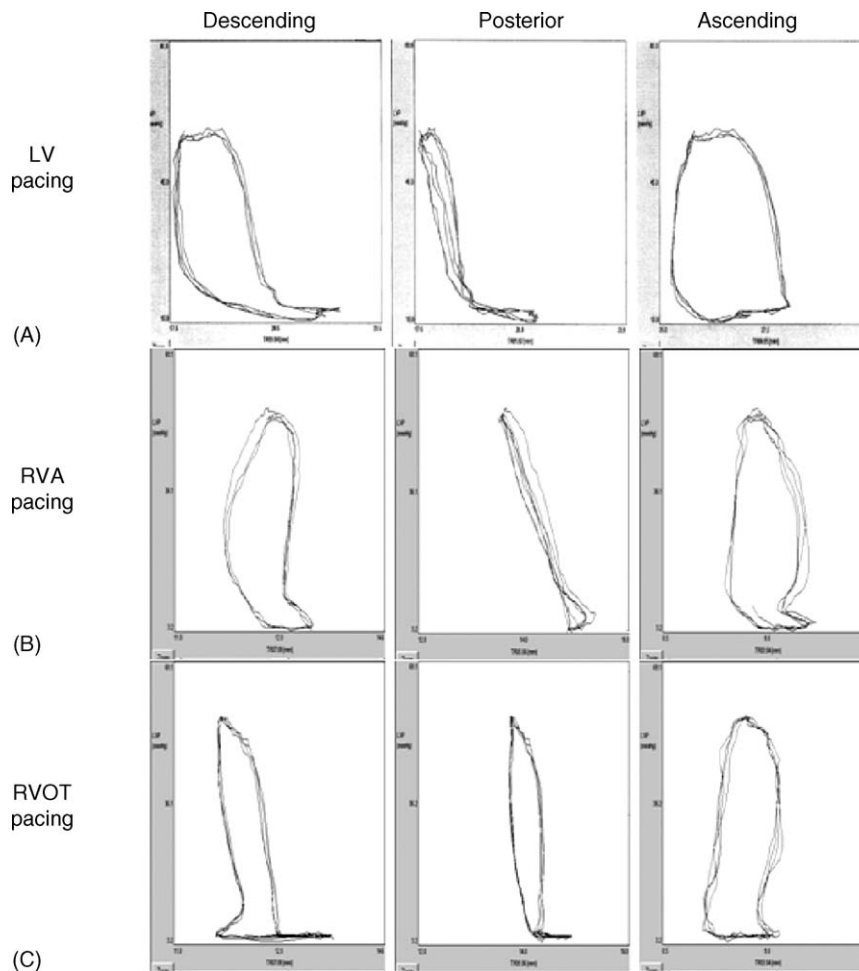


Fig. 11. Comparison of the pressure–dimension (P – D) loops of the descending, posterior and ascending segments during ventricular pacing. The longitudinal axis expresses LV pressure (mmHg), and horizontal axis is segment length (mm). Ventricular pacing of the LV (A), RV apex (B; RVA) and RV outflow tract (C; RVOT) decreased the integrated area of P – D loops and marked desynchronization was revealed. This is very evident when comparison is made to Fig. 10A and B showing NSR and atrial pacing.

loop segments and the posterior wall. Pacing of the RVOT caused an early onset of the descending segment and LV posterior wall shortening, which resulted in P – D loops that were out of phase with the beginning of LVP rise. Equally, RVA and LV pacing resulted in desynchronized P – D loops, resulting in a consistent loss of the twisting pattern of cardiac motion (Videos 3 and 4).

4. Discussion

The objective of this report was to measure the hemodynamic effects of different ventricular pacing sites, and determine if the resultant changes correlate with a dyssynchrony or disruption of the natural order of sequential contraction in the ventricular myocardial band of the helical heart [10]. This study did not intend to compare regional stimulus locations, so that no effort was made to search for the best site of unipolar stimulation.

The accumulated data (a) confirmed the established adverse hemodynamic effects of ventricular pacing from either the right or left ventricle on cardiac index, systolic and diastolic left ventricular function measured by peak (+) dP/dt

and (–) dP/dt , regional pressure–dimension loops, PRSW and end-systolic elastance, (b) established the natural pattern of sequential muscular contraction responsible for normal twisting, and (c) demonstrated how regional disruption of this pattern explains the mechanisms of asynchronous ventricular shortening.

This study sampled alternative pacing sites, a choice that stems from Wiggers suggestion in 1925 [22] that RVA pacing causes asynchronous ventricular contraction and is less effective than supraventricular activation. Recent evidence shows how RVA pacing alters dispersion of electrical and mechanical activation [23] and produces histopathological changes and asymmetric thickness of the left ventricular wall during chronic deterioration of left ventricular function [24–26]. Despite this recognition of how asynchrony of contracting myocardial segments deteriorates global performance, specific mechanisms that explain the adverse influence of pacing on ventricular structure are currently limited and conjectural, because the impact of pacing on function within normal spatial architecture has not yet been established.

This study had two objectives. First, this novel underlying myocardium architecture issue was addressed by focusing upon anatomic elements within the ventricular myocardial

band of the helical heart described by Torrent-Guasp [11], where the scrolled cardiac muscular structures contain two simple loops that start at the pulmonary artery and end at the aorta. These structural components include a circumferential basal loop that surrounds the left and right ventricles, and then becomes an oblique double helix to form the apical loop, comprising the descending segment and ascending segments [12,15]. Second, the sequential contraction in the continuous ventricular myocardial band was established by recording the orderly movement within the myocardial band by Fourier analysis in nuclear medicine studies [27] and subsequently reproduced in these sonomicrometer studies that recorded shortening in different spatial regions during movement that initially emanate from supraventricular and then ventricular stimulation. The natural role of sequential contraction was recorded and visualized by video, and corresponded to magnetic resonance imaging (MRI) study characterization of suspected fiber angle orientation responsible for twisting and untwisting of the apex for thickening and suction [28,29].

This report focuses upon establishing a sequence of temporal shortening of the apical loop segments of the band during sinus rhythm and atrial stimulation and demonstrates how disruption of this pathway by interrupting the supraventricular conduction by focal ventricular stimulation (RV apex, outflow tract or LV) changes the sequence. Regional pressure-segmental loops were recorded to define how each region contributed to organized or disorganized contraction.

During a normal sequential functional mechanism, shortening started initially in the endocardial side of the antero-septal wall of the left ventricle comprised of the descending segment, proceeded after a delay of 14 ± 8 ms to the LV posterior wall, and subsequently initiated shortening of the epicardium representing the ascending segment after a 86 ± 14 ms delay after endocardial wall shortening to correspond to the peak (+)dP/dt wave during ventricular ejection. Additionally, the ascending shortening phase continued for 110 ± 24 ms after the end of the descending segment shortening, an interval that corresponded to rapid left ventricular pressure deceleration while left ventricular suction occurs. The normal organization during NSR was quantified by pressure–dimension loops, and this pattern continued during supraventricular atrial pacing to demonstrate coordinated contributions of synchronous shortening of all spatial segments during left ventricular ejection. The twisting nature of this integration was recorded by video visualization as shown in Videos 1 and 2.

In contrast, RVA, RVOT and LV pacing produced marked aberration in the pressure–dimension loop, as shown in Fig. 11. The onset of shortening for each segment is out of order when compared with supraventricular rhythm and thus impaired the synchronous spatial twisting movement required for the ejection and suction phase, as shown in Videos 3–5. These asynchronous shortening abnormalities became evident by reductions in size and integrated loop areas in P–D loops, thus indicating less effective movement of the tested descending, posterior and ascending segments. The hemodynamic consequence was the less effective cardiac function, compared with findings after supraventricular stimulation. The cause was the inappropriate timing of ventricular stimulation, an event quantified by comparison

against the correct timing that followed supraventricular initiation of the pacing impulse.

While asynchrony and relative ineffectiveness of ventricular stimulation is clear from the data output, comparison of effectiveness different sites of ventricular stimulation (RVA, RVOT and LV) was not the objective of the present study. The natural pathways of sequential shortening along the myocardial band was demonstrated by following the organized shortening during sinus rhythm, and the data defines why atrial stimulation is preferable to inciting a current from the ventricular site. Such demonstration of the anatomic framework of fiber pathways along the helical heart fiber arrangement of the myocardial band that is responsible for organized shortening, makes it questionable if techniques of unipolar or even bipolar stimulation can ever be capable of generating an electrical stimulation site that can produce a synchronous contraction.

In conclusion, this study employs prior knowledge of the spatial architecture of cardiac construction to quantify why unipolar ventricular stimulation causes asynchrony. Disruption of the natural sequence of organized shortening along the myocardial band is the responsible mechanism for dyssynchrony after ventricular pacing. Identification of how normal pathways cause powerful sequential contraction, coupled with mapping of how these organized foci are impaired by isolated ventricular stimulation may provide a future framework to test effectiveness in subsequent studies of ventricular stimulation of the next heart beat.

References

- [1] Bogaert J, Rademakers FE. Regional nonuniformity of normal adult human left ventricle. *Am J Physiol Heart Circ Physiol* 2001;280(2):H610–20.
- [2] Varma C, Sharma S, Firoozi S, McKenna WJ, Daubert JC. Atrioventricular pacing improves exercise capacity in patients with heart failure and intraventricular conduction delay. *J Am Coll Cardiol* 2003;41(4):582–8.
- [3] Boerth RC, Covell JW. Mechanical performance and efficiency of the left ventricle during ventricular stimulation. *Am J Physiol* 1971;221(6):1686–91.
- [4] Buckingham TA, Candinas R, Attenhofer C, Van Hoeven H, Hug R, Hess O, Jenni R, Amann FW. Systolic and diastolic function with alternate and combined site pacing in the right ventricle. *Pacing Clin Electrophysiol* 1998;21(5):1077–84.
- [5] Riedbauchova L, Fridl P, Kautzner J, Peichl P. Performance of left ventricular versus biventricular pacing in chronic heart failure assessed by stress echocardiography. *Pacing Clin Electrophysiol* 2004;27(5):626–31.
- [6] Spragg DD, Akar FG, Helm RH, Tunin RS, Tomaselli GF, Kass DA. Abnormal conduction and repolarization in late-activated myocardium of dyssynchronously contracting hearts. *Cardiovasc Res* 2005;67(1):77–86.
- [7] Badke FR, Boinay P, Covell JW. Effects of ventricular pacing on regional left ventricular performance in the dog. *Am J Physiol* 1980;238(6):H858–67.
- [8] Burkhoff D, Oikawa RY, Sagawa K. Influence of pacing site on canine left ventricular contraction. *Am J Physiol* 1986;251:H428–35.
- [9] Takagi Y, Dumpis Y, Usui A, Maseki T, Watanabe T, Yasuura K. Effects of proximal ventricular septal pacing on hemodynamics and ventricular activation. *Pacing Clin Electrophysiol* 1999;22(12):1777–81.
- [10] Castella M, Buckberg GD, Saleh S, Gharib M. Structure function interface with sequential shortening of basal and apical components of the myocardial band. *Eur J Cardiothorac Surg* 2005;27(6):980–7.
- [11] Torrent-Guasp F, Ballester M, Buckberg GD, Carreras F, Flotats A, Carrio I, Ferreira A, Samuels LE, Narula J. Spatial orientation of the ventricular muscle band: physiologic contribution and surgical implications. *J Thorac Cardiovasc Surg* 2001;122(2):389–92.
- [12] Buckberg GD, Coghlan HC, Torrent-Guasp F. The structure and function of the helical heart and its buttress wrapping. V. Anatomic and physiologic

- considerations in the healthy and failing heart. *Semin Thorac Cardiovasc Surg* 2001;13(4):358–85.
- [13] Buckberg GD. The structure and function of the helical heart and its buttress wrapping. II. Interface between unfolded myocardial band and evolution of primitive heart. *Semin Thorac Cardiovasc Surg* 2001;13(4):320–32.
- [14] Streeter DD. In: Berne IR, editor. *Handbook of physiology, the cardiovascular system*. Bethesda, MD: American Physiological Society; 1979. p. p61–112.
- [15] Buckberg GD, Clemente C, Cox JL, Coghlan HC, Castella M, Torrent-Guasp F, Gharib M. The structure and function of the helical heart and its buttress wrapping. IV. Concepts of dynamic function from the normal macroscopic helical structure. *Semin Thorac Cardiovasc Surg* 2001;13(4):342–57.
- [16] Torrent-Guasp F, Buckberg GD, Clemente C, Cox JL, Coghlan HC, Gharib M. The structure and function of the helical heart and its buttress wrapping. I. The normal macroscopic structure of the heart. *Semin Thorac Cardiovasc Surg* 2001;13(4):301–19.
- [17] Barin ES, Jones SM, Ward DE, Camm AJ, Nathan AW. The right ventricular outflow tract as an alternative permanent pacing site: long-term follow-up. *Pacing Clin Electrophysiol* 1991;14(1):3–6.
- [18] Giudici MC, Thornburg GA, Buck DL, Coyne EP, Walton MC, Paul DL, Sutton J. Comparison of right ventricular outflow tract and apical lead permanent pacing on cardiac output. *Am J Cardiol* 1997;79(2):209–12.
- [19] Bernheim A, Ammann P, Sticherling C, Burger P, Schaer B, Brunner-La Rocca HP, Eckstein J, Kiencke S, Kaiser C, Linka A, Buser P, Pfisterer M, Osswald S. Right atrial pacing impairs cardiac function during resynchronization therapy: acute effects of DDD pacing compared to VDD pacing. *J Am Coll Cardiol* 2005;45(9):1482–7.
- [20] Varma C, O'Callaghan P, Mahon NG, Hnatkova K, McKenna W, Camm AJ, Rowland E, Brecker SJ. Effect of multisite pacing on ventricular coordination. *Heart* 2002;87(4):322–8.
- [21] Glower DD, Spratt JA, Snow ND, Kabas JS, Davis JW, Olsen CO, Tyson GS, Sabiston DC, Rankin JS. Linearity of the Frank–Starling relationship in the intact heart: the concept of preload recruitable stroke work. *Circulation* 1985;71:994–1009.
- [22] Wiggers CJ. The muscular reactions of the mammalian ventricles to artificial surface stimuli. *Am J Physiol* 1925;73:346–78.
- [23] Little WC, Reeves RC, Arciniegas J, Katholi RE, Rogers EW. Mechanism of abnormal interventricular septal motion during delayed left ventricular activation. *Circulation* 1982;65(7):1486–91.
- [24] Adomian GE, Beazell J. Myofibrillar disarray produced in normal hearts by chronic electrical pacing. *Am Heart J* 1986;112(1):79–83.
- [25] Karpawich PP, Justice CD, Cavitt DL, Chang CH. Developmental sequelae of fixed-rate ventricular pacing in the immature canine heart: an electrophysiologic, hemodynamic, and histopathologic evaluation. *Am Heart J* 1990;119(5):1077–83.
- [26] Lee MA, Dae MW, Langberg JJ, Griffin JC, Chin MC, Finkbeiner WE, O'Connell JW, Botvinick E, Scheinman MM, Rosenqvist M. Effects of long-term right ventricular apical pacing on left ventricular perfusion, innervation, function and histology. *J Am Coll Cardiol* 1994;24(1):225–32.
- [27] Ballester-Rodes M, Flotats A, Torrent-Guasp F, Carrio-Gasset I, Ballester-Alomar M, Carreras F, Ferreira A, Narula J. The sequence of regional ventricular motion. *Eur J Cardiothorac Surg* 2006;29S:S139–44.
- [28] Jung B, Schneider B, Markl M, Saurbier B, Geibel A, Hennig J. Measurement of left ventricular velocities: phase contrast MRI velocity mapping versus tissue-Doppler-ultrasound in healthy volunteers. *J Cardiovasc Magn Reson* 2004;6(4):777–83.
- [29] Shapiro EP, Rademakers FE. Importance of oblique fiber orientation for left ventricular wall deformation. *Technol Health Care* 1997;5(1–2):21–8.

Appendix A. Supplementary data

Supplementary data associated with this article can be found, in the online version, at [doi:10.1016/j.ejcts.2006.02.053](https://doi.org/10.1016/j.ejcts.2006.02.053).